Heliyon

Received:
5 August 2017
Revised:
21 November 2017
Accepted:
3 January 2018

Cite as: Abdelilah Benallou, Habib El Alaoui El Abdallaoui, Hocine Garmes. C—C bond formation in the intramolecular Diels-Alder reaction of triene amides.
Heliyon 4 (2018) e00504.
doi: 10.1016/j.heliyon.2018.e00504

C—C bond formation in the intramolecular Diels-Alder reaction of triene amides

Abdelilah Benallou [a,*], **Habib El Alaoui El Abdallaoui** [a], **Hocine Garmes** [b,c]

[a] *Team of Chemoinformatics Research and Spectroscopy and Quantum Chemistry, Physical and Chemistry Lab, Faculty of Science, El Jadida, Morocco*

[b] *Laboratory of Bio-organic Chemistry, Department of Chemistry, Faculty of Science, El Jadida, Morocco*

[c] *University Chouaib Doukkali, B.P. 20, 2300, El Jadida, Morocco*

* Corresponding author.

E-mail address: abdo_benallou@yahoo.fr (A. Benallou).

Abstract

The mechanism nature of the intramolecular Diels–Alder reaction has been performed; and thus, the changes of C—C bond forming/breaking along IRC are characterized in this study. Conceptual DFT analyses of the most favorable adduct fused/exo shows that the flux electronic will take place from diene to dienophile moiety. Moreover, ELF topological analysis based on the electron density predicts that C—C bond is formed by the coupling of two pseudoradical centers generated at the most significant atoms of the molecules. However, C2 vs C3, also C1 and C4 interaction comes mainly from the global electron density transfer which takes place along the reaction. Two- stage one-step is the proposed mechanism of this reaction, the first stage aims for the formation of C2—C3 σ bond while the second stage aims for C1—C4 σ bond formation. Interestingly, the observed asynchronicity of this IMDA reaction due principally to the asymmetric reorganization of electron density at the most attractive centers.

Keywords: Theoretical chemistry, Physical chemistry, Organic chemistry

1. Introduction

Diels-Alder (DA) reaction is undoubtedly one of the most powerful tools in synthetic organic chemistry of six-membered carbocycles from diene and

http://dx.doi.org/10.1016/j.heliyon.2018.e00504

dienophiles frameworks [1, 2, 3, 4], since this reaction is considered as an important propelling of the organic reactions, one of the most noticeable roles of organic chemistry is to understand the bond forming and breaking processes along of the reaction. However, the development of theoretical approach of reactivity give a reliable comprehension of how reagents convert into products, via the transition state (TS), the basic objectives of a given chemistry approach is to analyze the changes in the observable quantum mechanics along the path of the reaction, using a reasonable calculation. Interestingly, to analyze the changes in mechanical quantum observable on the reaction path, mainly the reorganization of the electron density throughout the reaction path, the theoretical model of the evolution of the bonding [5] and the topological analysis of the electrons localization [6] are combined during this last decade and are actually used and are the most more attractive methods to analyze a mechanism of reaction, because these latter's are successively verified an appropriate tool for the studies of the organic reactions [7, 8, 9] and are a fascinating method to examine a reaction mechanism. However, and in order to shed light the IMDA reaction we have previously studied the role of solvent (water) and catalysts on the feasibility for intramolecular Diels-Alder chemical reactions of triene amide molecules to yield hexahydoindole [10, 11]. Importantly, the intramolecular Diels-Alder (IMDA) reaction is widely used for the construction of the cycles in a single synthetic process for the construction of six-membered rings [12, 13, 14, 15, 16, 17, 18]. That justifies the development of theoretical models for DA reaction, which involves a large number of the dienes and dienophiles. For that reason, the IMDA reaction to yield hexahydroindole is taken as the classic example of an organic reaction [19, 20]. In this context, the reaction pathway may be established using the internal reaction coordinate (IRC) method [21] on the potential energy surface (PES).

In order to comprehend the bonding formation along the reaction and to insight the nature of TS and mechanism processes, the combination of Conceptual DFT and ELF theory has been used to best characterizing the reaction pathway through optimized geometries for corresponding stationary points on the IRC path. Therefore, the molecular mechanism study of IMDA reaction has been realized. Moreover, triene-amide is a molecule constitutes in same time the diene (D) and dienophile (Dp) fragments also the Nitrile (CN) function has been substituted dienophile as an attractor of electron. Previously we have shown that exo/fused is the most favorable adduct of IMDA reaction to produce hexahydroindole (Fig. 1) [3, 22], then this study will be realized especially of this latter isomeric pattern.

2. Methods

DFT computations were carried out using the B3LYP exchange–correlation functional [23], together with the standard 6-31G(d,p) basis set [24]. The optimizations were carried out using the Berny analytical gradient optimization method [25]. The stationary points were characterized by frequency computations

http://dx.doi.org/10.1016/j.heliyon.2018.e00504

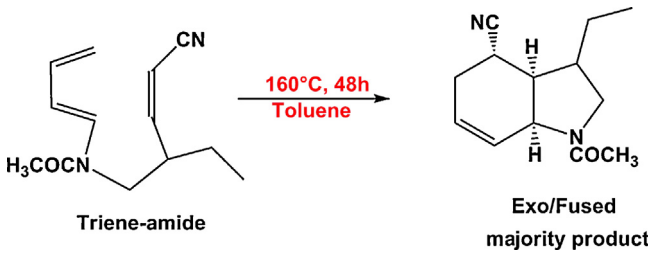

Fig. 1. Observed region-selectivity of the IMDA reactions of triene-amide.

in order to verify that the TS structure has one and only one imaginary frequency along of the IRC paths [26] using the second order Gonzalez–Schlegel integration method [27]. The electronic structures of stationary points were analyzed by the natural bond orbital (NBO) method [28] and by ELF topological analysis [6]. The ELF study was performed with the Multiwfn program [29] using the corresponding mono determinantal wavefunctions of the selected structures of the IRC. All computations were carried out with the Gaussian 09 suite of programs [30]. The global electrophilicity index, ω [31], is given by the following expression, $\omega = \mu^2/2\eta$, in terms of the electronic chemical potential μ and the chemical hardness η. Both quantities may be approached in terms of the one-electron energies of the frontier molecular orbital HOMO and LUMO, e_H and e_L, as $\mu = (e_H + e_L)/2$ and $\eta = (e_L - e_H)$ [32], respectively. Domingo et al. have proposed a new descriptor, the nucleophilicity index, N [33], based on the HOMO energies obtained within the Kohn–Sham scheme [34], and defined as $N = E_{HOMO(Nu)} - E_{HOMO(TCE)}$. The nucleophilicity is referred to tetracyanoethylene (TCE), as a reference. Where f_k^- and f_k^+ are the Fukui functions for nucleophilic and electrophilic attacks, respectively [35].

3. Results and discussion

Determining the nature of mechanism reaction and understanding the changes of C—C bond formation/breaking in the IMDA reactions of triene-amide along of IRC, lead us to effectuate an analysis of physicochemical character of triene-amide molecule, then to evaluate a mechanistic study of the reaction between diene and dienophile frameworks in molecule to describe the C—C bond-formation step in IMDA reactions. Equally, an ELF bonding analysis along the C—C bond-formation pathway of this reaction is carried out in order to establish the nature and changes of electron density along of the bond formation/breaking.

3.1. Analysis of the Conceptual DFT (CDFT) indices of triene-amide

It is very important to identify the characteristics of triene-amide (A) molecule to better understanding their reactivity, then to know the distribution of the global and local electrophilicity and nucleophilicity indices within the molecule. For instance,

http://dx.doi.org/10.1016/j.heliyon.2018.e00504

Table 1. B3LYP/6-31G(d,p) electronic chemical potential μ, chemical hardness η, global electrophilicity ω and global nucleophilicity N.

μ (eV)	η (eV)	ω (eV)	N (eV)
−3.51	4.62	1.33	3.29

the electronic chemical potential μ is associated with the feasibility of a system to exchange electron density with the environment at the ground state, the chemical hardness η can be thought as a resistance of a molecule to exchange electron density with the environment, while the electrophilicity ω index and nucleophilicity N index encompasses the tendency of an electrophile to acquire or a nucleophile to donate an extra amount of electron density, respectively. The CDFT indices [36] of the triene-amide compound are given in Table 1.

Following the results in Table 1 we can remark that this molecule is powerful nucleophilic character such as the global nucleophilic index N is very advanced to compare with the global electrophilic index ω, in good agreement with the biggest chemical potential, −3.51 eV. The high nucleophilic character of this molecule is a consequence of the high nucleophilic character of the butadiene framework. Note that in the IMDA reaction it is very difficult to characterize the donor or/and acceptor regions because diene and dienophile fragments are attached by a tether, so this intramolecular reagent must be divided to an appropriate moiety of diene and dienophile to better studying. At this point and in order to highlight the electrophilic and nucleophilic centers, rather, evaluate the withdrawing and releasing groups fragment within the intramolecular triene amide, at this end, we will calculate the regional descriptors of fragments. Thus, the results are given in Table 2.

The results in Table 2 note that the diene moiety has the predominant nucleophilic and electrophilic character compared to the dienophile fragment such as $N_D(2.98) > N_{Dp}(0.31)$ also $\omega_D(0.72) > \omega Dp(0.61)$, so in this case is difficult to identify the character of each fragment. therefore, at this point we will calculate the global electron density transfer (GEDT) [37] in the TS, this latter has been detected in the Hessian matrix by one and only imaginary frequency of fused isomer adduct,

Table 2. Regional nucleophilicity and electrophilicity of diene and dienophile fragment.

Diene (D) Fragment				Dienophile (Dp) Fragment			
Σf^+	ω (eV)	Σf^-	N (eV)	Σf^+	ω (eV)	Σf^-	N (eV)
0.545	0.72	0.904	2.98	0.455	0.61	0.096	0.32

http://dx.doi.org/10.1016/j.heliyon.2018.e00504

and thus, the estimated GEDT in TS is about, +0.11e and −0.11e for diene and dienophile, respectively, the sign + indicates that the electronic fluxes take place from dienes to dienophiles fragments. Therefore, the diene framework behaves as the nucleophile and the ethylene framework as the electrophile.

3.2. Mechanistic study of the reaction between diene and dienophile frameworks in molecule triene-amide

An analysis of the potential energy surface (PES) associated with the C—C bond-formation step in the IMDA reaction of triene-amide indicates that C—C bond-formation processes probably take place through high asynchronous processes, because the presence of the asymmetric nucleophilic and electrophilic centers, similarly, the GEDT between diene and dienophile fragments in TS, is about 0.11e, indicates that the IMDA reaction is a moderate polarity. To confirm that this IMDA reaction is asynchronous, we will calculate the bond orders by using Wiberg index in the NBO analysis [28] of TS (Fig. 2). An analysis of the TS structure, lead us to conclude that C2—C3 single bond distance is very short to compare of C1—C4 single bond in which 2.10 Å and 2.39 Å, respectively. In this sense, Wiberg index confirms the same conclusion which this reaction is extensively high asynchronous such as the bond orders are 0.30 for C1—C4 and 0.42 for C2—C3 bonds, subsequently C1—C4 and C3—C2 bonds formation are totally distinct. Note that the bond order of C1—C4 bond distance is very small compared to C2—C3 bond, confirm that this bond is formed lately; however C2—C3 bond will be formed firstly. In consequence, this reaction is asynchronous and is not concerted process. Simultaneously, these important consequences will help us to identify the mainly electrophilic and nucleophilic

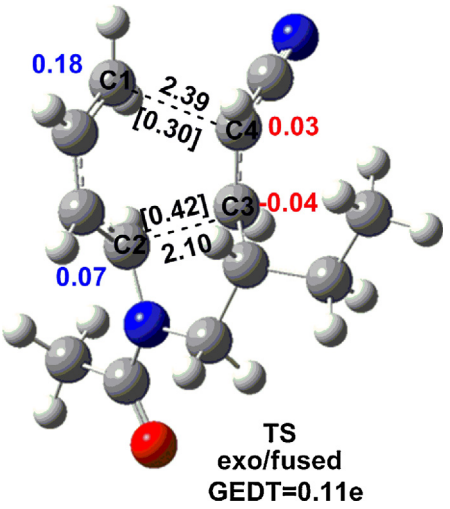

Fig. 2. Local electrophilic (in red) and nucleophilic (in blue) Fukui functions $f_k^{\pm}$, bond distances (Å) and bond orders (Wiberg index) of exo/fused transition structure.

http://dx.doi.org/10.1016/j.heliyon.2018.e00504

centers to best interpreting the most attractive sites. In this context, we have calculated the local electrophilic and nucleophilic centers of dienophile and diene fragment respectively. So, according the results noted in Fig. 2, we have shown that the most significant sites are C1 (0.18) and C4 (0.03), followed by C2 (0.07) and C3 (−0.04) centers, respectively.

3.3. ELF bonding analysis of the IRC path of the C—C bond-formation step in the intramolecular reaction of triene-amide

In this paragraph, we will try to characterize the mechanism of reaction and will justify the processes of compound formation, then, to identify the distribution of electronic density with the progress of the reaction along of bond breaking/formation [38], and in particular to understand the asynchronous bond-formation in this IMDA reaction. In this fact, a topological analysis of the ELF of some significant points of the IRC path associated with the C—C bond-formation step in the intramolecular reaction of triene-amide was carried out for the fused/exo adduct (majority product), and thus the population electronic of each atom along the reaction has been detected carefully in this study. Therefore, the attractor positions for the most relevant points associated with the formation of the C1—C4 and C2—C3 single bond, are shown in Fig. 3, and the electronic density of the more relevant ELF valence basins of selected points along the IRC of the one-step mechanism are listed in Table 3. It is interesting to note that, the basins are the areas where the chance to find an electronic pair is maximum, while this descriptor [39] is adapted to the Lewis bonding model.

In this work, the discussion will be focalized particularly for the most relevant and attractor points such as C1, C2, C3, C4, Ca and Cb. Thus, we have illustrated that ELF analysis for R (Reagent) while the bonds distance *d(C1—C4) = 2.77* Å *and d (C2—C3) = 2.51* Å, two pairs {V(C1,Ca); V′(C1,Ca)} and {V(Cb,C2);V′(Cb,C2)} disynaptic basins has been shown of diene fragment associated with the two double bonds of C1—Ca and Cb—C2 integrating 3,32e and 3,44e respectively, similarly in dienophile fragment, two V(C3,C4) and V′(C3,C4) disynaptic basins are located at double bonds C3—C4, integrating 1.71e, while the disynaptic basin V(Ca,Cb) associated with the single bond Ca—Cb reaching an electron population of 2.28e.

At point I, *d(C1—C4) = 2.62 and d(C2—C3) = 2.36* Å, the ELF topology designates almost the same results noted in reagent with a few changes in electron population such as has been diminished slightly for three pairs disynaptic basins {V(C1,Ca);V′(C1,Ca)}, {V(Cb,C2);V′(Cb,C2)} and {V(C3,C4);V′(C3,C4)}; whose the population electronic integrate 3.27e, 3.38e and 3.32e respectively, however the disynaptic basin of V(Ca,Cb) associated with the single bond Ca—Cb

http://dx.doi.org/10.1016/j.heliyon.2018.e00504

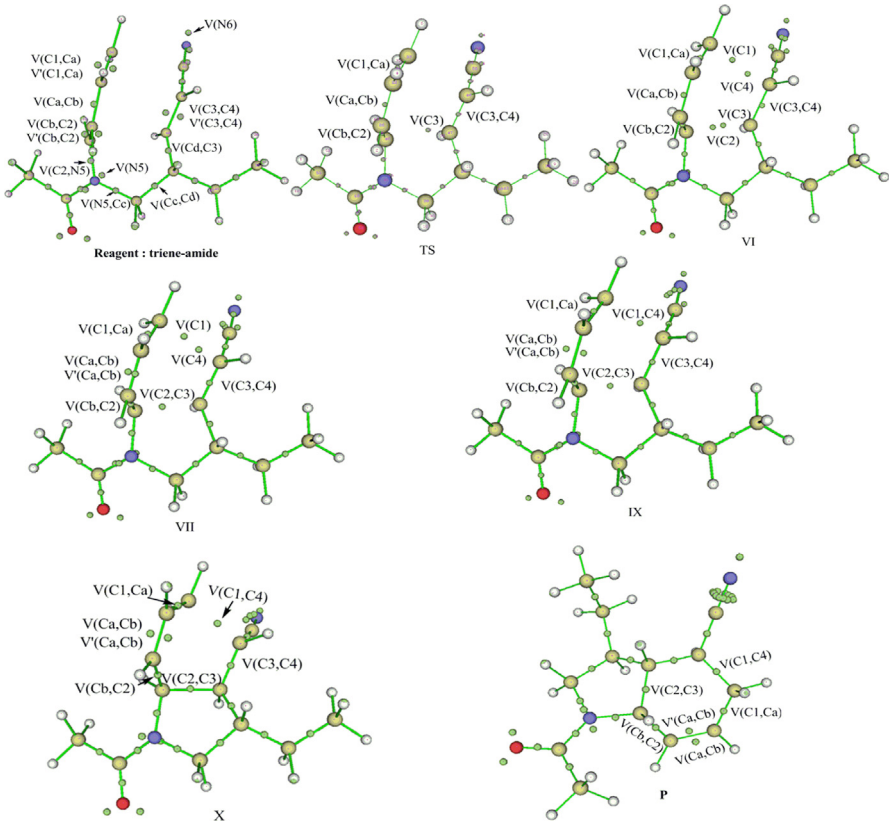

Fig. 3. ELF attractors V(M) and V(M,N) of some selected points (R, TS, VI, VII, IX, X and P) of the IRC related to the formation of the new C—C single bond in the IMDA reaction of triene-amide.

has been a little increased from 2.28e to 2.35e, indicates that this bond begins to transform slowly to double bonds.

At point II, *d(C1—C4) = 2.54 and d(C2—C3) = 2.28* Å, several changes take place in this point such as the two V(C1,Ca) and V′(C1,Ca) disynaptic basins associated with C1—Ca π bond has transformed to one V(C1,Ca) disynaptic basin integrating 3.22e, indicates that this bond becomes single in clear agreement with Diels-Alder rules [12], while the electronic population of the two pairs {V(Cb,C2); V′(Cb,C2)} and {V(C3,C4);V′(C3,C4)} disynaptic basins have been slightly diminished to 3.34e and 3.31e respectively, justifies that these double bonds will disappear finally to single bond, hence the ELF of V(Ca,Cb) integrates 2.42e reveal that Ca—Cb σ bond profits to more electron density along of the reaction coordinate.

At point III of the IRC, *d(C1—C4) = 2.47 and d(C2—C3) = 2.19* Å, the most relevant results noted at this point is that Cb-C2 becomes single bond, at this point the electron density of V(Cb,C2) disynaptic basin decreases to 3.28e, in addition, the electron population of the V(C1,Ca) disynaptic basin and the two V(C3,C4); V′(C3,C4) disynaptic basins proceed to more decrease of 3.15e and 3.32e respectively, whereas the population electronic of V(Ca,Cb) disynaptic basin

http://dx.doi.org/10.1016/j.heliyon.2018.e00504

Table 3. Valence basin populations of the most relevant points calculated from the ELF of intramolecular Diels-Alder reaction of triene-amide, associated with the C1-C4 and C2-C3 bonds formation step. Bond order (Wiberg index) and GEDT in *e* (NBO).

Points	R	I	II	III	IV(TS)	V	VI	VII	VIII	IX	X	P
d(C1-C4)	2.77	2.62	2.54	2.47	2.39	2.31	2.27	2.23	2.15	2.06	1.96	1.57
d(C2-C3)	2.51	2.36	2.28	2.19	2.10	2.01	1.96	1.92	1.84	1.76	1.70	1.56
BO(C1,C4)	0.06	0.10	0.15	0.21	0.30	0.41	0.47	0.53	0.63	0.72	0.80	0.97
BO(C2,C3)	0.08	0.15	0.21	0.30	0.42	0.55	0.61	0.67	0.77	0.84	0.89	0.97
GEDT	0.06	0.08	0.09	0.10	0.11	0.11	0.11	0.11	0.11	0.10	0.09	0.05
V(C1)	–	–	–	–	–	–	0.24	0.33	0.41	–	–	–
V(C2)	–	–	–	–	–	0.56	0.64	–	–	–	–	–
V(C3)	–	–	–	–	0.35	0.48	0.53	–	–	–	–	–
V(C4)	–	–	–	–	–	0.41	0.48	0.53	0.65	–	–	–
V(C1,Ca)	3.32	3.27	3.22	3.15	3.03	2.91	2.62	2.49	2.33	2.22	2.14	1.98
V′(C1,Ca)	3.32	3.27	–	–	–	–	–	–	–	–	–	–
V(Ca,Cb)	2.28	2.35	2.42	2.53	2.71	2.98	3.10	3.18	3.31	3.39	1.83	1.81
V′(Ca,Cb)	–	–	–	–	–	–	–	3.18	3.31	3.39	1.62	1.74
V(Cb,C2)	3.44	3.38	3.34	3.28	3.20	2.54	2.44	2.36	2.24	2.16	2.11	2.04
V′(Cb,C2)	3.44	3.38	3.34	–	–	–	–	–	–	–	–	–
V(C2,N5)	1.79	1.79	1.78	1.77	1.75	1.74	1.73	1.72	1.70	1.68	1.67	1.62
V(N5,Cc)	1.60	1.59	1.60	1.61	1.60	1.60	1.61	1.61	1.61	1.62	1.62	1.60
V(Cc,Cd)	1.92	1.92	1.92	1.92	1.91	1.91	1.91	1.90	1.90	1.90	1.89	1.90
V(Cd,C3)	2.05	2.06	2.06	2.04	2.02	2.00	1.98	1.97	1.95	1.94	1.93	1.89
V(C1,C4)	–	–	–	–	–	–	–	–	–	1.22	1.36	1.79
V(C2,C3)	–	–	–	–	–	–	–	1.29	1.47	1.60	1.68	1.88
V(C3,C4)	1.71	3.32	3.31	3.32	3.02	2.51	2.41	2.31	2.17	2.07	2.01	1.88
V′(C3,C4)	1.63	3.32	3.31	3.32	–	–	–	–	–	–	–	–
V(N5)	0.91	0.88	0.86	0.84	0.82	0.80	0.78	0.76	0.74	0.72	0.72	0.91
V(N6)	3.28	3.28	3.29	3.29	3.29	3.30	3.29	3.30	3.29	3.28	3.27	3.24

increase significantly to 2.53e along of the IRC. Conversely, the other monosynaptic and disynaptic basins noted in Table 3 are not much changed.

At point IV (TS), *d(C1—C4) = 2.39 and d(C2—C3) = 2.10* Å, this point constitutes the TS that represents the biggest GEDT along of the intrinsic reaction coordinate, the ELF shows the formation of the first V(C3) monosynaptic basin in atom C3 of dienophile fragment that contains the population electronic of 0.35e, indicate that the first factor of the new C—C formation really begin, similarly, the two V(C3,C4); V′(C3,C4) disynaptic basins are merged into new and one V(C3,C4) disynaptic basin of electronic density 3.02e, explain that C—C π bond

http://dx.doi.org/10.1016/j.heliyon.2018.e00504

has been transformed lately to C—C σ bond, especially for the two disynaptic basins V(C1,Ca) and V(Cb,C2), in which the population electronic have decreased regularly with the progress of the reaction, integrating 3.03e and 3.20e, respectively. On the contrary, the electronic density of V(Ca,Cb) disynaptic basin has been slightly increased with the advancement of reaction. Interestingly, the new bond formation is not yet started.

At point V, *d(C1—C4) = 2.31 and d(C2—C3) = 2.01* Å, in this point the two new monosynaptic are created, V(C2) and V(C4) associated with C2 and C4 atoms which a population electronic of 0.56e and 0.41e respectively, in this sense the V(C3) monosynaptic basin is strengthened in point of view of the electronic density to 0.48e, this is indicator of the new C—C σ bond formation will be started in the upcoming point, hence the population electronic of V(C1,Ca), V(Cb,C2) and V(C3,C4) disynaptic basins still decrease sequentially until the end of reaction, integrating 2.91e, 2.54e and 2.51e respectively, indicate that a large quantities of electron density has been transferred from C1—Ca, Cb—C2 and C3—C4 π bonds to form the new C—C σ bond.

At point VI, *d(C1—C4) = 2.27 and d(C2—C3) = 1.96* Å, herein the formation of the new V(C1), V(C2), V(C3) and V(C4) monosynaptic basins of the most attractor carbons atoms is complete, whose a population electronic of 0.24e, 0.64e, 0.53e and 0.48e respectively. Interestingly, the V(C3) and V(C2) monosynaptic basins contain the higher electronic density, therefore are probably will react firstly. While the population electronic of the V(C1,Ca), V(Cb,C2) and (C3,C4) disynaptic basins continue to decreases to 2.62e, 2.44e, 2.41e respectively, otherwise the V(Ca,Cb) disynaptic basin acquire more density electronic along the IRC, 3.10e.

At point VII, *d(C1—C4) = 2.23 and d(C2—C3) = 1.92* Å, the ELF shows that the V(C2) and V(C3) monosynaptic basins are merged to a new V(C2,C3) disynaptic basin with an electronic population of 1.29e, confirm the formation of the first bond between C2 (diene) and C3 (dienophile) atoms, whereas the other bond between C1 and C4 atoms is not yet started, but are profit to more charge electronic, because the population electronic of V(C1) and V(C4) monosynaptic basins increases to 0.33e and 0.53e, respectively, another news is noted at this point V(Ca,Cb) disynaptic basin associated with Ca—Cb single bond in which split to V(Ca,Cb) and V′(Ca,Cb) disynaptic basin, integrate 3.18e; Ca—Cb being double bond finally, while the electronic population of V(C1,Ca), V(Cb,C2) and (C3,C4) disynaptic basins still decreases to 2.49e, 2.36e and 2,31e, respectively.

At point VIII, *d(C1—C4) = 2.15 and d(C2—C3) = 1.84* Å, V(C1) and V(C4) monosynaptic basins achieved a maximum electron density of 0.41e and 0.65e, However, C2—C3 σ new bond has reached to more charge in which the electron density of V(C2,C3) disynaptic basin increases to 1.47e, although the electronic

http://dx.doi.org/10.1016/j.heliyon.2018.e00504

population of attractors V(C1,Ca), V(Cb,C2) and (C3,C4) disynaptic basins are always decreasing to 2.33e, 2.24e and 2.17e, respectively, whilst V(Ca,Cb) disynaptic basin increases another time to 3.31e.

At point IX, *d(C1—C4) = 2.06 and d(C2—C3) = 1.76* Å, the second most relevant changes in this IMDA reaction take place. The two V(C1) and V(C4) monosynaptic basins present in diene and dienophile fragments merge into a new disynaptic basin, V(C1,C4), which integrates 1.22e, indicating that the formation of the second C1—C4 single bond begins (see Fig. 3). The population electronic of the V(C1,Ca), V(Cb,C2) and V(C3,C4) disynaptic basins decrease newly to 2.22e, 2.16e and 2.07e, respectively, whereas the electronic population of the V(Ca,Cb) disynaptic basin increases to 2.39e.

At point X, *d(C1—C4) = 1.96 and d(C2—C3) = 1.70* Å, ELF topological shows that the new C—C σ bond continues to profit more electronic population in which for V(C1,C4) and V(C2,C3) disynaptic basins 1.36e and 1.68e respectively, indicate that the C2—C3 single bond is practically already formed. Whereas, the electronic population of V(C1,Ca), V(Cb,C2) and V(C3,C4) disynaptic basins still decrease to 2.14e, 2.11e and 2.10e respectively, the same consequences have been noted for the electronic density of V(Ca,Cb) disynaptic basin that has diminished to 1.83e after reach a maximum value in point IX.

In the product, *d(C1—C4) = 1.57 and d(C2—C3) = 1.56* Å, the new C—C single bonds formation are totally completed in the product and the electronic population of several basins becomes stable, while the GEDT achieve a feeble value 0.05e, thus the IRC is complete and the most stable adduct is formed.

In addition, V(Cd,C3), V(C2,N5), V(N5,Cc) and V(Cc,Cd) disynaptic basins, then V(N5) and V(N6) monosynaptic basins do not have more change along the IRC.

Consequently, this ELF analysis study we permit to follow the change of electron density along the IRC, thus we have shown that the charge transferred is very feeble in the reagent CT = 0.06e and is slightly increased along the progress of the reaction until reach a maximum value CT = 0.11e in points IV (TS), V and VI, then has been diminished little by little until the end of reaction, confirm that this reaction is a moderate polarity. It is interesting to remark that, the formation of new C—C σ bond appears highly asynchronous, the Wiberg index calculation justifies that C2—C3 σ bond formation is always advanced to that C1—C4 σ bond formation as shown in Table 3; Wiberg index (C2—C3) > Wiberg index (C1—C4). A conclusion has been retained in this study, IMDA reaction passes through two-stage one-step [40], the first stage is located between the reagent and point VII, C 2—C3 σ bond will be formed, while in the second stage between point VIII and product, C1—C4 σ bond is completely formed.

http://dx.doi.org/10.1016/j.heliyon.2018.e00504

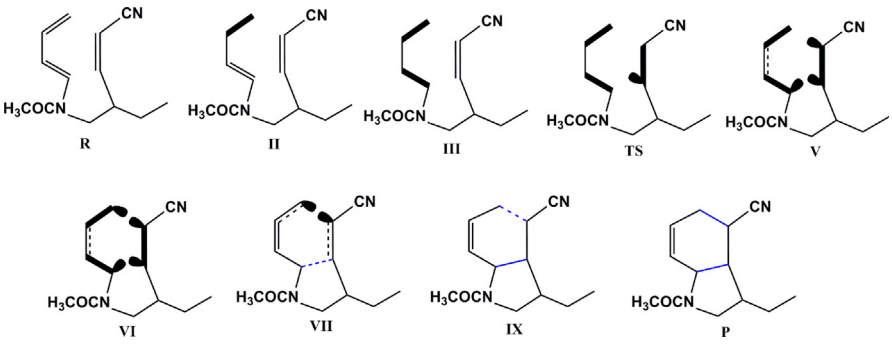

Fig. 4. Bonding changes demonstration at the selected points (R, II, III, TS, V, VI, VII, IX and P) involved in the IMDA reaction of triene-amide. Lines represent bonding V(M,N) disynaptic basins, and ellipses represent non-bonding V(M) monosynaptic basins. Filled lines (in blue) indicate new V(M,N) disynaptic basins formation.

These findings clearly proven that the reactivity observed of this IMDA reaction is controlled generally by the electron density and not by the local nucleophilicity or electrophilicity noted in Fig. 2, thus, a complete representation of the bonding changes along the selected points involved in this IMDA reaction is given in Fig. 4, whereas a graphic representation of the energy profile along the two-stage one-step mechanism of the IMDA reaction of triene-amide, illustrate the relative position of the selected points along the IRC, is presented in Fig. 5. Subsequently, some appealing conclusions can be drawn from this study the IMDA reaction of triene-amide takes place through a pseudodiradical species, two-stage one-step to form hexahydroindole as summarized in Fig. 6.

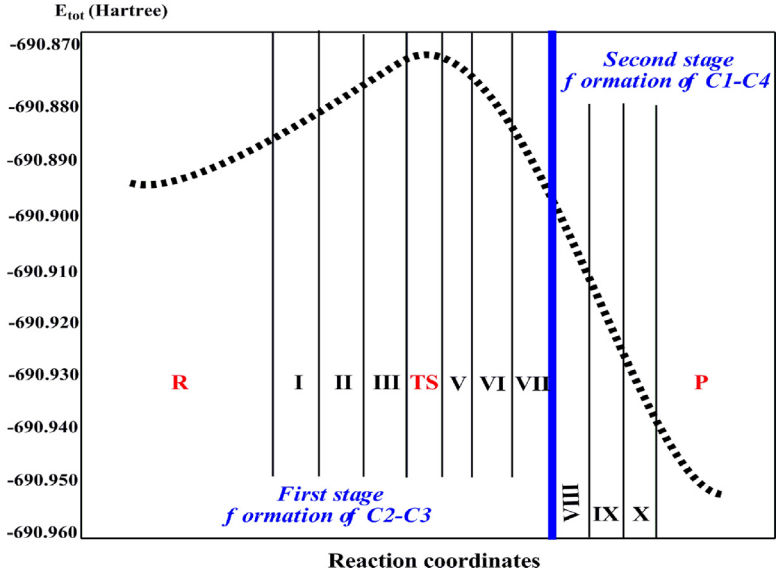

Fig. 5. A complete representation of the energy profile, in Hartree, of the IMDA reaction of triene-amide.

http://dx.doi.org/10.1016/j.heliyon.2018.e00504

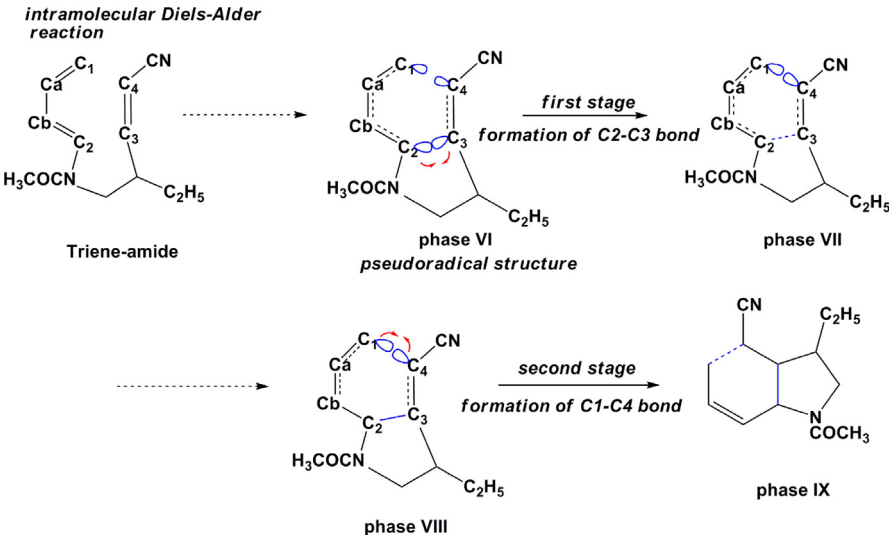

Fig. 6. C—C bond formation model in the Intramolecular-Diels–Alder reaction of triene-amide along of two-stage one-step mechanism.

The chosen points of the IRC used in the ELF topological analysis are totally represented in Fig. 5. The vertical blue line divides the IRC into the two distinct stages associated with the formation of the C1—C4 and C2—C3 single bonds. It is worth nothing to remark that TS is located in the first stage, reveals that this reaction is not concerted process.

4. Conclusion

The cycloaddition intramolecular Diels-Alder (IMDA) reaction of triene-amide has been studied using DFT methods at the B3LYP/6-31G** and an ELF topological analysis of selected points along of the IRC in order to characterize the bonding changes in the C—C bond formation process has been performed. For this IMDA reaction, two-stage one-step mechanisms have been found, equally, ELF topological analysis we permit to conclude that this reaction is made between the most electrophilic and nucleophilic centers of diene and dienophile fragment to yield a pseudodiradical species. As a result, the electron-reorganization at the pseudoradical species generated by the GEDT along this reaction, which involving asymmetric electrophilic and nucleophilic centers associated with the most favorable sites, is responsible for the observed asynchronicity. Thus, the first stage is associated with the C2—C3 σ bond formation in which C2 and C3 atoms have the higher electron density, while the second stage corresponds to C1—C4 σ bond formation where C1 and C4 atoms have the small electron density. However, this IMDA reaction is controlled generally by the electron density and not by the local nucleophilicity or electrophilicity indices. Importantly, the ELF analyses give a deep comprehension and explanation of IMDA mechanism reaction and equally provide a complete characterization of the electron density changes along C—C bond formation.

http://dx.doi.org/10.1016/j.heliyon.2018.e00504

Declarations

Author contribution statement

Abdelilah Benallou, Habib El Alaoui El Abdallaoui, Hocine Garmes: Conceived and designed the experiments; Performed the experiments; Analyzed and interpreted the data; Contributed reagents, materials, analysis tools or data; Wrote the paper.

Competing interest statement

The authors declare no conflict of interest.

Funding statement

This research did not receive any specific grant from funding agencies in the public, commercial, or not-for-profit sectors.

Additional information

No additional information is available for this paper.

References

[1] J. Soto-Delgado, L.R. Domingo, R. Contreras, Quantitative characterization of group electrophilicity and nucleophilicity for intramolecular Diels–Alder reactions, Org. Biomol. Chem. 8 (2010) 3678.

[2] (a) R.S. Paton, S.E. Steinhardt, C.D. Vanderwal, K.N. Houk, Unraveling the mechanism of cascade reactions of Zincke aldehydes, J. Am. Chem. Soc. 133 (2011) 3895;
(b) H. Garmes, Degree Thesis, University of Chouaib, Doukkali, 1995.

[3] A. Benallou, H. Garmes, E.H. El Alaoui, Theoretical study of the regioselectivity in the intramolecular Diels–Alder reaction of the molecule triene amide, Mor. J. Chem. 2 (2014) 181. http://revues.imist.ma/index.php?journal=morjchem&page=article&op=view&path%5B%5D=1912.

[4] A. Benallou, H. Garmes, N. Knouzi, E.H. El Alaoui, Elucidation of the regioselectivity in hetero diels-alder reaction by utilization of theoretical approaches, Phys. Chem. News 72 (2014) 85. http://www.pcnjournal.com/147211_1898.htm.

[5] X. Krokidis, B. Silvi, M.E. Alikhani, Topological characterization of the isomerization mechanisms in XNO (X = H, Cl), Chem. Phys. Lett. 292 (1998) 35.

http://dx.doi.org/10.1016/j.heliyon.2018.e00504

[6] A. Savin, B. Silvi, F. Colonna, Topological analysis of the electron localization function applied to delocalized bonds, Can. J. Chem. 74 (1996) 1088.

[7] L.R. Domingo, S. Emamian, M. Salami, Understanding the molecular mechanism of [3 + 2] cycloaddition reaction of benzonitrile oxide toward an *N*-vinylpyrrole derivative with the aid of ELF topological analysis, J. Phys. Org. Chem. 29 (2016) 368.

[8] P.S.V. Kumar, V. Raghavendra, V. Subramanian, Bader's theory of atoms in molecules (AIM) and its applications to chemical bonding, J. Chem. Sci. 128 (2016) 1527.

[9] D.B. Chesnut, A topological study of bonding in the Al2H2 and Al2H4 hydrides, Chem. Phys. 321 (2006) 269.

[10] A. Benallou, E.H. El Alaoui, H. Garmes, Effect of hydrogen bonding on the intramolecular cycloaddition DielseAlder reaction of triene-amide in an aqueous solution (case of a single molecule of water), Tetrahedron 72 (2016) 76.

[11] A. Benallou, E.H. El Alaoui, H. Garmes, A conceptual DFT approach towards analysing feasibility of the intramolecular cycloaddition Diels-Alder reaction of triene amide in Lewis acid catalyst, J. Chem. Sci. 128 (2016) 1489.

[12] O. Diels, K. Alder, Synthesen in der hydroaromatischen Reihe, Justus Liebigs Ann. Chem. 460 (1928) 98.

[13] R.B. Woodward, R. Hoffmann, The conservation of orbital symmetry, Angew. Chem. Int. Ed. Engl. 8 (1969) 781.

[14] J.D. Winkler, Tandem dielsminus sign Alder cycloadditions in organic synthesis, Chem. Rev. 96 (1996) 167.

[15] W. Carruthers, Some Modern Methods of Organic Synthesis, 2nd ed., Cambridge University Press, Cambridge, U.K, 1978.

[16] W. Carruthers, Cycloaddition Reactions in Organic Synthesis, Pergamon, Oxford, 1990.

[17] Z. Chen, M.L. Trudell, Chemistry of 7-Azabicyclo[2.2.1]hepta-2.5-dienes, 7-Azabicyclo[2.2.1]hept-2-enes, and 7-azabicyclo[2.2.1] heptanes, Chem. Rev. 96 (1996) 1179.

[18] F. Finguelli, A. Tatichi, The Diels-Alder reaction. Selected Practical Methods, Wiley, New York, 2002.

 http://dx.doi.org/10.1016/j.heliyon.2018.e00504

[19] E.W.G. Diau, S. De Feyter, A.H. Zewail, Femtosecond dynamics of retro Diels–Alder reactions: the concept of concertedness, Chem. Phys. Lett. 304 (1999) 134.

[20] C. Corminboeuf, T. Heine, J. Weber, The change of aromaticity along a Diels-Alder reaction path, Org. Lett. 5 (2003) 1127.

[21] C. Gonzalez, H.B. Schlegel, Reaction path following in mass-weighted internal coordinates, J. Phys. Chem. 94 (1990) 5523.

[22] A. Benallou, E.H. El Alaoui, H. Garmes, Theoretical examination of the stereoselectivity of the intramolecular cycloaddition Diels-Alder reaction of triene-amide, IJIAS 8 (2014) 685–696. http://www.issr-journals.org/abstract.php?=14-218-14.

[23] (a) C. Lee, W. Yang, R.G. Parr, Development of the Colle-Salvetti correlation-energy formula into a functional of the electron density, Phys. Rev. B 37 (1988) 785;
(b) A.D. Becke, Density-functional thermochemistry. III. The role of exact exchange, J. Chem. Phys. 98 (1993) 5648.

[24] W.J. Hehre, L. Radom, P.V.R. Schleyer, J.A. Pople, Ab Initio Molecular Orbital Theory, Wiley, New York, 1986.

[25] H.B. Schlegel, Modern Electronic Structure Theory, 1st ed., World Scientific Publishing, Singapore, 1994.

[26] K. Fukui, Formulation of the reaction coordinate, J. Phys. Chem. 74 (1970) 4161.

[27] C. Gonzalez, H.B. Schlegel, Improved algorithms for reaction path following: higher-order implicit algorithms, J. Chem. Phys. 95 (1991) 5853.

[28] A.E. Reed, L.A. Curtiss, F. Weinhold, Intermolecular interactions from a natural bond orbital, donor-acceptor viewpoint, Chem. Rev. 88 (1988) 899.

[29] L. Tian, C. Feiwu, Multiwfn: a multifunctional wavefunction analyzer, J. Comp. Chem. 33 (2012) 580–592.

[30] M.J. Frisch, et al., Gaussian, Revision A.02, Gaussian Inc, Wallingford, CT, 2009.

[31] R.G. Parr, L.V. Szentpaly, S. Liu, Electrophilicity index, J. Am. Chem. Soc. 121 (1999) 1922.

[32] R.G. Parr, R.G. Pearson, Absolute hardness: companion parameter to absolute electronegativity, J. Am. Chem. Soc. 105 (1983) 7512.

 http://dx.doi.org/10.1016/j.heliyon.2018.e00504

[33] L.R. Domingo, P. Pérez, The nucleophilicity N index in organic chemistry, Org. Biomol. Chem. 9 (2011) 7168.

[34] W. Kohn, L. Sham, Self-consistent equations including exchange and correlation effects, J. Phys. Rev. 140 (1965) 1133.

[35] R. Contreras, P. Fuentealba, M. Galván, P. Perez, A direct evaluation of regional Fukui functions in molecules, Chem. Phys. Lett. 304 (1999) 405.

[36] L.R. Domingo, M.R. Gutiérrez, P. Pérez, Applications of the conceptual density functional theory indices to organic chemistry reactivity, Molecules 21 (2016) 748.

[37] L.R. Domingo, A new CC bond formation model based on the quantum chemical topology of electron density, RSC Adv. 4 (2014) 32415.

[38] E. Chamorro, M. Duque, C. Cárdenas, J. Santos, W. Tiznado, P. Fuentealba, Condensation of the highest occupied molecular orbital within the electron localization function domains, J. Chem. Sci. 117 (2005) 419.

[39] B. Silvi, The synaptic order: a key concept to understand multicenter bonding, J. Mol. Struct. 614 (2002) 3.

[40] L.R. Domingo, J.A. Saez, R.J. Zaragoza, M. Arno, Understanding the participation of quadricyclane as nucleophile in polar [2σ + 2σ + 2π] cycloadditions toward electrophilic π molecules, J. Org. Chem. 73 (2008) 8791–8799.

 http://dx.doi.org/10.1016/j.heliyon.2018.e00504